Lnc-TMEM132D-AS1 Confers Acquired Resistance to Osimertinib in Non-Small-Cell Lung Cancer

Nan Wang
Chongqing Medical University
Qilin Zhao
Chongqing Medical University
Yutang Huang
Chongqing Medical University
Chunjie Wen
Chongqing Medical University
Yaji Li
Chongqing Medical University
Lanxiang Wu (lxwu@cqmu.edu.cn)
Chongqing Medical University

Research Article

Keywords: Lnc-TMEM132D-AS1, Acquired resistance, Osimertinib, NSCLC, ENTPD1

Posted Date: June 17th, 2022

DOI: https://doi.org/10.21203/rs.3.rs-1747227/v1

Abstract

Objective: Acquired resistance is a major obstacle to the therapeutic efficacy of osimertinib in non-small-cell lung cancer (NSCLC). Current knowledge about the role of long non-coding RNAs (lncRNAs) in this phenomenon is insufficient. Here, we aim to identify candidate lncRNAs associated with acqured resistance to osimertinib in NSCLC, and explore the role and underlying mechanism of one of these lncRNAs, lnc-TMEM132D-AS1.

Methods and Results: RNA Sequencing (RNA-Seq) and quantitative real-time PCR (qPCR) were used to screen and validate the differentially expressed lncRNAs between osimertinib-sensitive and -resistant NSCLC cell lines. Lnc-TMEM132D-AS1 was screened out, and was found to be upregulated in the osimertinib-resistant NSCLC cell lines as well as the plasma of NSCLC patients. Results from CCK-8, colony formation, flow cytometry assays showed that lnc-TMEM132D-AS1 knockdown significantly increased the sensitivity of osimertinib-resistant NSCLC cells to osimertinib. After identifying the cytoplasmic localization of lnc-TMEM132D-AS1, a functional lnc-TMEM132D-AS1-miRNA-mRNA interaction network and protein-protein interaction (PPI) network were constructed to analyze its putative target genes and biological functions. Using qPCR and TISIDB database analysis, ectonucleoside triphosphate diphosphohydrolase-1 (ENTPD1) was confirmed to be a target mRNA of lnc-TMEM132D-AS1, and was associated with tumor infiltration of immunosuppressive cells and poor prognosis in patients with NSCLC.

Conclusion: In summary, lnc-TMEM132D-AS1 plays a crucial role in osimertinib resistance. It may serve as a prognostic biomarker and a potential therapeutic target for acquired resistance to osimertinib in NSCLC.

Introduction

Lung cancer is the most frequently diagnosed cancer and is the leading cause of cancer-related death worldwide. According to WHO statistics, about 2.2 million people are diagnosed with lung cancer and 1.7 million people die from it each year. Non-small cell lung cancer (NSCLC) is the most common type of lung cancer, which accounts for approximately 85% of all cases (1). Most patients are in the middle or advanced stage when they are diagnosed, so the five-year survival rate is only about 15% (2). NSCLC is a highly heterogeneous disease, often driven by well characterized oncogenic “driver” mutations, the best known of which are common alterations in epidermal growth factor receptor (EGFR) (3). Consequently, the EGFR tyrosine kinase inhibitors (EGFR-TKIs) are used in clinical practice, resulting in better outcomes than platinum-based chemotherapy in patients with EGFR-mutated NSCLC (4).

Osimertinib is the first Food and Drug Administration (FDA)-approved third-generation EGFR-TKI, and is approved as first-line therapy for advanced EGFR-mutated NSCLC, regardless of T790M mutation status (5). However, despite the excellent clinical efficacy, the development of acquired resistance to osimertinib is inevitable after about 10 months treatment (6). The mechanisms of this phenomenon are very

complex, which can be broadly grouped into EGFR-dependent or EGFR-independent mechanisms, including altered EGFR signaling pathway, aberrant activation of bypass and downstream signaling pathways, and histological trans-formation. However, the underlying mechanisms still remain unknown in 53–69% of cases after first-line treatment, as well as in 30–60% of cases after second-line treatment (7).

Long non-coding RNAs (lncRNAs) are a kind of non-coding RNAs (ncRNAs) that are longer than 200 nucleotides, and are mainly involved in regulation of cellular physiological and pathological activities. In recent years, more and more reports have revealed that lncRNAs are involved not only in cancer progression, but also in the development of chemoresistance (8). Up to now, several studies have proved that lncRNAs may play crucial roles in the development of acquired osimertinib resistance. For example, CRNDE, MSTRG.292666.16, and HIF1A-AS2 are overexpressed in osimertinib resistant NSCLC cells, which can decrease osimertinib sensitivity through sponging microRNAs (miRNAs) or interacting with RNA binding proteins (9–11). However, only very few of them have been examined so far, and the biological processes between more lncRNAs and acquired osimertinib resistance remain largely unknown.

In this study, we first performed RNA sequencing (RNA-Seq) to identify the differentially expressed lncRNAs between osimertinib-resistant NSCLC cells (HCC827/OR and H1975/OR) and their parental cells (HCC827 and H1975). After qPCR validation, lnc-TMEM132D-AS1 was found to be significantly upregulated in both osimertinib-resistant NSCLC cell lines and the plasma samples from patients. Lnc-TMEM132D-AS1 knockdown significantly reduced osimertinib sensitivity *in vitro*. Then, a functional lnc-TMEM132D-AS1-miRNA-mRNA network was constructed, Gene Ontology (GO) terms, Kyoto Encyclopedia of Genes and Genomes (KEGG) pathways, and protein-protein interaction (PPI) analyses were used to explore the potential biological functions of lnc-TMEM132D-AS1 targeted mRNAs. Finally, one of the lnc-TMEM132D-AS1 target mRNAs, ectonucleoside triphosphate diphosphohydrolase-1 (ENTPD1) was screened out, and was revealed to be associated with both tumor infiltration of immunosuppressive cells and poor prognosis of NSCLC patients. Our results may provide a new molecular biomarker and therapeutic target for acquired resistance to osimertinib in NSCLC.

Materials And Methods

Cell culture

Human NSCLC HCC827 cells (EGFR exon 19 deletion) and H1975 cells (EGFR L858R and T790M) were purchased from the Cellular Institute of the Cellular Institute of Chinese Academy of Science (Shanghai, China). NSCLC cells with acquired resistance to osimertinib (HCC827/OR and H1975/OR) were established by exposing HCC827 and H1975 cells to a gradually increasing concentration of osimertinib (Target Mol, USA) for about 10 months. Then the final resistant cells were stably tolerant to growth in complete medium containing 0.5μM osimertinib. All the cells were cultured in RPMI-1640 (Gibco, USA) medium supplemented with 10% fetal bovine serum (FBS) (Gibco, USA) and 100 U/mL of penicillin and streptomycin (Beyotime, China) at 37^{o}C in a humidified atmosphere of 5% CO_2 and 95% air. Two weeks before the experiments, osimertinib was removed to prevent drug interference. Cell lines were regularly

tested for mycoplasma, and were authenticated at source by STR profiling, morphology (ATCC) and DNA profiling (ECACC).

Patients and clinical sample collection

This study was approved by the Ethics Committee Board of Chongqing Medical University, Chongqing, P.R.China (No. 2017009), and was registered with the Chinese Clinical Trial Registry (No. ChiCTR1800014660). A total of 25 NSCLC patients that underwent first-line osimertinib therapy, including 15 gefitinib-sensitive patients and 10 gefitinib-acquired resistant patients were enrolled in this study. Written informed consents were obtained from all of them. The patients were given osimertinib at a daily dose of 80 mg until tumor progression, the objective response to treatment was assessed with the Response Evaluation Criteria in Solid Tumors (RECIST) version 1.1. Acquired resistance to osimertinib was defined by using the Jackman criteria (12). Details of patients are listed in Table S1. The peripheral blood samples of these patients were collected in EDTA tubes, centrifuged (2,000 g for 10 min) at 4°C within 4h, and were stored at liquid nitrogen.

Cell variability assay

Cells were seeded in 96-well plates at a density of 2×10^3 cells per well. After 24h culture, cells were treated with various concentrations of osimertinib (0.01-1μM) for 72h, followed by addition of 10μL Cell Counting Kit-8 (CCK-8) solution (Dojindo Molecular Technologies, Japan) and incubation for an additional 4h at 37°C. The absorbance was recorded at 450nm with a spectrophotometer (Thermo-Fisher Scientific, USA). Osimertinib sensitivity was estimated using half-inhibitory concentration (IC_{50}) values (defined as the drug concentration resulting in a 50% reduction of viability compared with the control).

Colony formation assay

Cells were plated into 6-well plates at 1×10^3 cells per well, and cultured in the presence of 0.5μM osimertinib for 72h. Then the drugs were washed away and the medium was changed every 3 days for 2 weeks. Colonies were fixed with 4% paraformaldehyde for 15min and stained with 1% crystal violet staining solution (Beyotime, China) for 10min in the dark. Photographs of all the colonies were acquired under a light microscope (DM3000, Leica, Germany).

Cell apoptosis assay

Cells were seeded into 6-well plate and treated with 0.5μM osimertinib or DMSO for 72h. All cells including suspending in the media were collected, incubated with 5μL of annexin V-FITC and 5μL of propidium iodide (PI) for 15min in the dark at 4°C. Apoptosis was analyzed by flow cytometry (Beckman Coulter, USA).

Cell cycle analysis

Cells were seeded into 6-well plate and treated with 0.5μM osimertinib or DMSO for 72h. All cells were collected and resuspended in 1mL pre-cold 70% ethanol and incubated at 4^{o}C overnight. After centrifuging at 1000 rpm for 5min, 1mL DNA staining solution and 10μL permeabilization solution (MultiSciences Biotech Co, China) were added, then the cells were incubated at room temperature for 30min in the dark. Cell cycle was determined by flow cytometry (Beckman Coulter, USA).

Protein isolation and western blot analysis

Cells were lysised by RIPA lysis buffer (Sigma, USA), and the total protein was extracted and quantified using the Pierce bicinchoninic acid (BCA) protein assay kit (Thermo Fisher Scientific, USA). Proteins were separated by 8% SDS-PAGE and transferred to the polyvinylidene fluoride (PVDF) membranes. After being blocked with 5% BSA at room temperature for 2h, membranes were incubated at 4°C overnight with the primary antibodies as follows: Akt (1:1,000, Cell Signaling Technology), phospho-Akt (Ser473) (1:2,000, Cell Signaling Technology), phosphatidylinositol 3-kinase (PI3K) (1:1,000, Cell Signaling Technology), phospho-PI3K (Tyr458/199) (1:1,000, Cell Signaling Technology), EGFR (1:1,000, Abcam), phospho-EGFR (Tyr1068) (1:500, Abcam), and GAPDH (1:5,000, Bioss). After 1h of incubation with horseradish peroxidase (HRP)-conjugated secondary antibody (Cell Signaling Technology, USA), immunoreactive bands were detected by ECL substrate kit (Thermo Fisher Scientific,USA).

RNA isolation and quantitative real-time PCR (qPCR)

Total RNA was extracted from cells using the RNA-Quick Purification Kit (YiShan Biotech,China), and the separation of the nuclear and cytoplasmic RNA was performed using a Paris kit (Thermo Fisher Scientific, USA), the percentages in fractions were analyzed using the following formula: $2^{-Ct\ (nuclear)}/(2^{-Ct\ (nuclear)} + 2^{-Ct\ (cytoplasm)})$, and $2^{-Ct\ (cytoplasm)}/(2^{-Ct\ (nuclear)} + 2^{-Ct\ (cytoplasm)})$. The cell-free RNA (cfRNA) was extracted from plasma of NSCLC patients using the miRNeasy Serum/Plasma Kit (Qiagen, USA). The isolated RNA was reverse-transcribed into cDNA using the Takara reverse transcription kit (Takara Bio, Japan). qPCR was performed using TB Green® Premix Ex Taq™ II (Takara Bio, Japan). The primer sequences used in this study are shown in Table S2. Relative gene expression levels were analyzed using the $2^{-\triangle\triangle CT}$ method as a ratio relative to the U6 or GAPDH levels in each sample (13).

RNA sequencing (RNA-Seq)

Total RNA from NSCLC cells was extracted using TRIzol reagent (Invitrogen, USA) and treated with a Turbo DNA-free Kit (Thermo Fisher Scientific, USA) to degrade the remaining DNA. The RNA was subsequently purified using a Ribo-Zero Gold Kit (Illumina, USA) and RNase R (Epicenter, USA). RNA integrity was evaluated using the Agilent 2100 Bioanalyzer (Agilent Technologies, Santa Clara, CA, USA). Samples with RNA integrity number ≥7 were used for the subsequent analysis. The libraries were constructed using TruSeq Stranded Total RNA with Ribo-Zero Gold according to the manufacturer's instructions. These libraries were then sequenced on the Illumina platform (HiSeq™ 2500 or another

platform) and 150/125 base pair (bp) paired-end reads were generated. All the sequencing procedures and analyses were performed in OEbiotech (Shanghai, China).

Oligonucleotides and transfection

Three lnc-TMEM132D-AS1-specific siRNAs were used to knock down lnc-TMEM132D-AS1, and a non-silencing siRNA (si-NC) oligonucleotide was used as a negative control (GenePharma, Shanghai, China). For transfections, 1×10^6 cells/well were plated into a 6-well plate, and siRNAs were transfected into the cells using Lipofectamine 3000 (Invitrogen, CA, USA) following the manufacturer's protocol. The transfected cells were harvested after 72h, and the transfection efficiency was determined by qPCR, and the lnc-TMEM132D-AS1-specific siRNA sequences are listed in Table S2.

Co-expression network construction

A lnc-TMEM132D-AS1-mRNA co-expression network was constructed based on the correlations between the lnc-TMEM132D-AS1 and differentially expressed mRNAs, using the algorithm of Pearson's Correlation. The network construction procedures include: (i) preprocess data: the same coding gene with different transcripts take the median value as the gene expression values, without special treatment of lncRNA expression value; (ii) screen data: remove the subset of data according to the lists that show the differential expression of lncRNA and mRNA; (iii) calculate the Pearson correlation coefficient and use R value to calculate the correlation coefficient of PCC between lncRNA coding genes; and (iv) screen by Pearson correlation coefficient, select the part where PCC>0.8 as meaningful and draw the network by Cytoscape version 3.7.1 (http://www.cytoscape.org/).

Lnc-TMEM132D-AS1-miRNA-mRNA network construction

Lnc-TMEM132D-AS1-miRNA interactions were first predicted using DIANA TOOLS (diana.imis.athena-innovation.gr/). Then, Targetscan (http://www.targetscan.org/) and miRDB (http://www.mirdb.org/) were used to predict the potential miRNA target mRNAs. Finally, a lnc-TMEM132D-AS1-miRNA-mRNA network by matching lnc-TMEM132D-AS1-miRNA and miRNA-mRNA pairs were established, and the graph was created using Cytoscape version 3.7.1.

GO and KEGG pathway analyses

GO terms and KEGG pathway analyses were applied to determine the main functions and related signaling pathways of the potential target mRNAs of lnc-TMEM132D-AS1. To accomplish these analyses, cluster Profiler 3.0.1 in R (http://www.bioconductor.org/packages/release/bioc/html/clusterProfiler.html) was applied.

Protein-protein interaction (PPI) analysis

PPI interaction networks for the mRNAs from the lnc-TMEM132D-AS1-miRNA-mRNA network were constructed using the Search Tool for the Retrieval of Interacting Genes (STRING) database

(http://stringdb.org/). The mRNAs were typed into the database and download the high-resolution bitmaps according to the official medium confidence given by String, and the possible relationships was detected with a minimum required interaction score of 0.4, removing disconnected nodes. The hub genes in the PPI networks were identified using CytoHubba, a plugin in Cytoscape software.

TISIDB Database Analysis

TISIDB database (http://cis.Hku.hk/TISIDB/) is a portal for analyzing tumor and immune cell interactions that integrates multiple heterogeneous data types (14). We analyze the correlation between ENTPD1 expression and tumor-infiltrating immunosuppressive cells via this platform.

Kaplan-Meier plotter analysis

The Kaplan-Meier plotter (http://kmplot.com/analysis/) offers a means of readily exploring the impact of a wide array of genes on patient survival in different types of cancer. It was used to explore the association between the expression of lnc-TMEM132D-AS1 or ENTPD1 and clinical outcomes of patients, and to perform a prognostic analysis based on ENTPD1 expression levels in relevant immune cell subgroups. With the purpose to assess prognostic value of a specific gene, the patient samples were divided into two cohorts according to the median expression of the gene (high *vs* low expression). Hazard ratios (HRs) of 95% confidence intervals (CIs) and the log-rank *P*-value were calculated.

Statistical Analysis

DESeq (2012) R package was applied to identify differentially expressed lncRNAs and differentially expressed mRNAs with setting the threshold of *P* value < 0.05 and foldchange > 2 or foldchange < 0.5 (absolute value of log2 ratio ≥ 1). Hierarchical cluster analysis was performed to demonstrate the expression pattern of lncRNAs and mRNAs in different samples. GO terms and KEGG pathway analyses were respectively performed using R based on the hypergeometric distribution. The Pearson correlation coefficient (PCC) was calculated to evaluate the co-expression relationships between differentially expressed lncRNAs and mRNAs. The co-expressed genes with PCC > 0.8 and a correlation P value < 0.05 were identified as statistically significant. One-way analysis of variance and two-tailed student's *t*-tests were performed to analyze the differences between sets of data using SPSS statistical software (Version 17.0, USA). Data are presented as mean±standard error of the mean (SEM). Values of $P<0.05$ were regarded statistically significant.

Results

Validation of osimertinib resistance in HCC827/OR and H1975/OR cell lines

Two NSCLC cell lines with acquired resistance to osimertinib, HCC827/OR and H1975/OR, were established from their parental cells. CCK-8 assay showed that after 72h of osimertinib exposure, the IC_{50} values were 0.0032μM and 0.0036μM in HCC827 and H1975 cells, respectively. As expected, HCC827/OR

and H1975/OR cells showed significantly decreased sensitivity to osimertinib, with the IC_{50} values of 3.91μM and 5.13μM, respectively (Figure 1A and 1B). Similarly, colony formation assay also indicated that the colony formation abilities of HCC827/OR and H1975/OR cells were significantly higher than their parental sensitive cells (Figure 1C and 1D). After osimertinib exposure, the HCC827 and H1975 cells exhibited both apoptosis and cell cycle arrest, while HCC827/OR and H1975/OR cells were not affected (Figure 1E and 1F). Moreover, unlike their parental cells, osimertinib-resistant cells maintained high phosphorylation levels of EGFR and downstream signaling components even following treatment with osimertinib (Figure 1G). These results indicate that the HCC827/OR and H1975/OR cells are more resistant to osimertinib than their parental cell lines.

Identification and validation of the differentially expressed lncRNAs between osimertinib-sensitive and -resistant NSCLC cell lines

To explore the role of lncRNAs in osimertinib resistance in NSCLC, we first examined the differentially expressed lncRNAs between osimertinib-resistant cells and their parental cells using RNA-Seq (Figure 2A). A total of 64678 lncRNAs were identified from our NSCLC cells, and the majority of them were from intergenic regions (42%), exonic of protein-coding genes (21%), and introns of protein-coding genes (20%) (Figure 2B). Our results showed that 427 lncRNAs were differentially expressed between HCC827/OR and HCC827 cells, consisting of 212 upregulated and 215 downregulated lncRNAs. While 471 lncRNAs were differentially expressed between H1975/OR and H1975 cells, consisting of 218 upregulated and 253 downregulated lncRNAs. Of these, 17 lncRNAs were consistently upregulated and 15 lncRNAs were consistently downregulated in both osimertinib-resistant cells compared with their parental cells (Figure 2C, Table 1). As previously reported, chromosomal abnormality often occurs in NSCLC, and some lncRNAs have been recognized as important regulators of chromosome stability (15,16). Therefore, we investigated the chromosomal localization of these differentially expressed lncRNAs. As shown in Figure 2D, these lncRNAs were significantly enriched in chromosome 1 and 12.

To validate the RNA-Seq results, we randomly selected 20 differentially expressed lncRNAs for qPCR, and found seven of them were consistent with the RNA-Seq data. Compared with the parental sensitive cells, four lncRNAs (lnc-TMEM132D-AS1, lnc-XLOC_003074, lnc-AC006064.5, and lnc-ZNF213-AS1) were significantly upregulated both in HCC827/OR and H1975/OR cells, whereas three lncRNAs (lnc-GAS5, lnc-AC007952.4, and lnc-SNHG29) were markedly downregulated in two resistant cell lines (Figure 2E).

Upregulated lnc-TMEM132D-AS1 reduces sensitivity to osimertinib in NSCLC cells

According to the results mentioned above, lnc-TMEM132D-AS1 was the most significantly upregulated lncRNA after acquired resistance to osimertinib in NSCLC cells. To preliminary explore the clinical significance of lnc-TMEM132D-AS1, we analyzed its expression in lung cancer tissues, as well as the relationship between its expression and clinical outcomes in lung cancer patients using The Cancer Genome Atlas (TCGA) database. The results showed that the expression of lnc-TMEM132D-AS1 was significantly higher in lung cancer tissues than in normal tissues (P<0.001). The patients with high lnc-

TMEM132D-AS1 expression showed decreased overall survival (OS) and progression-free survival (PFS) (both *P*<0.001) (Figure 3A and 3B). Additionally, we found that lnc-TMEM132D-AS1 was located on chromosome 12. Therefore, we selected lnc-TMEM132D-AS1 for further investigation. Firstly, we determined the expression of lnc-TMEM132D-AS1 in cultured osimertinib-sensitive and -resistant NSCLC cells, as well as in the plasma samples of osimertinib-sensitive and -resistant NSCLC patients. Compared to the parental sensitive cells, significantly elevated level of lnc-TMEM132D-AS1 was observed not only in the whole-cell lysates, but also in the culture supernatants of HCC827/OR and H1975/OR cells (Figure 3C and 3D). Similarly, the level of lnc-TMEM132D-AS1 in the plasma of NSCLC patients with acquired resistance to osimertinib was about 8-fold higher than that of osimertinib-sensitive patients (Figure 3E). These data provide evidence that lnc-TMEM132D-AS1 is upregulated in NSCLC cells with acquired resistance to osimertinib both *in vitro* and *in vivo*, and is a potential biomarker for resistance to osimertinib therapy.

Then, we observed the the influence of lnc-TMEM132D-AS1 on osimertinib sensitivity in NSCLC cells. After silencing the expression of lnc-TMEM132D-AS1 in HCC827/OR cells, we found that the cell survival rate and colony formation capacity after osimertinib exposure were significantly decreased, the osimertinib-induced apoptosis was markedly increased, and cell cycle was obviously arrested in G2/M phase (Figure 3F-I). These data suggest that lnc-TMEM132D-AS1 can significantly reduce the osimertinib sensitivity and is a potential target for overcoming osimertinib resistance.

The potential mechanisms of lnc-TMEM132D-AS1 in osimertinib resistance

In order to explore the molecular mechanism of lnc-TMEM132D-AS1 in osimertinib resistance, we firstly determined its subcellular localization, because the functional mechanisms of lncRNAs are dependent on their subcellular distribution (17). We found that lnc-TMEM132D-AS1 was mainly expressed in the cytoplasm of NSCLC cells (Figure 4A), indicating that it might play important roles in modulating mRNA stability, translation and signalling pathways through acting as a sponge of miRNAs (18). Therefore, we set out to explore the potential miRNAs interacting with lnc-TMEM132D-AS1, as well as their potential mRNA targets.

Firstly, we screened the differentially expressed mRNAs between osimertinib-sensitive and -resistant NSCLC cells using RNA-Seq, and selected 576 mRNAs which showing similar expression tendencies in both paired cell lines, then calculated the Pearson correlation coefficient (PCC) between these mRNAs and lnc-TMEM132D-AS1 to evaluate the co-expression relationships. A total of 215 mRNAs with PCC > 0.8 and a correlation *P* value < 0.05 were chosen to build the co-expression network (Figure 4B). Subsequently, using DIANA TOOLS, Targetscan, and miRDB databases, we found 148 miRNAs with binding capacity to lnc-TMEM132D-AS1, as well as their 756 potential target mRNAs. Accordingly, we took the intersection of the selected 215 differentially expressed mRNAs with the predicted 756 potential target mRNAs. As a result, we constructed the lnc-TMEM132D-AS1-miRNA-mRNA interaction network, including 125 miRNAs and 162 target mRNAs (Figure 4C).

Then, we performed GO and KEGG analyses to explore the putative functions of these 162 target mRNAs. We analyzed all three GO aspects: biological processes, cellular composition, and molecular function. The top 15 dysregulated GO processes are shown in Figure 4D. In the biological processes subgroup, the top three dysregulated GO processes were immune response, inflammatory response, and positive regulation of cell proliferation. In the cellular composition subgroup, the top three dysregulated GO processes were extracellular environment, extracellular region, and integral component of plasma membrane. While in the molecular function subgroup, the top three dysregulated GO processes were ATP binding, identical protein binding, and extracellular matrix structural constituent. Interestingly, one of these target mRNAs, ENTPD1, was included in three GO terms, which were immune response, extracellular environment, as well as ATP binding. For KEGG analysis, the top 20 dysregulated pathways are shown in Figure 4E. Of these, the environmental information processing, ascorbate and aldarate metabolism, and pentose and glucuronate interconversions were the most enriched pathways.

To further mine the resistance-associated genes, we performed PPI network analysis based on these 162 target mRNAs, and identified some hub genes, of which the top 10 were CDH1, TIMP3, FBN1, DLJ4, CDH2, GJA1, NGFR, ENTPD1, IGF2, and NKX2-5. Most of these hub genes have been shown to take part in chemoresistance. For example, FBN1, GJA1, and IGF2 were related to cisplatin resistance (18-20), while TIMP3, CDH2, NGFR, and ENTPD1 were involved in resistance to sorafenib, 5-fluorouracil, icotinib and cytarabine, respectively (21-24). These findings support that, at least partially, lnc-TMEM132D-AS1 might play a role in osimertinib resistance in NSCLC.

The expression of ENTPD1, a target mRNA of lnc-TMEM132D-AS1, correlates with tumor-infiltrating immunosuppressive cells and poor prognosis in patients with NSCLC

Given that GO analysis showed that one of the lnc-TMEM132D-AS1 target mRNAs, ENTPD1, were similarly related to three GO terms, and PPI analysis also indicated that ENTPD1 was one of the hub genes, so we selected it for further study. ENTPD1 also referred to as CD39 and NTPDase, is a Ca^{2+} and Mg^{2+}-dependent integral cell membrane molecule, which phosphohydrolases extracellular ATP to produce AMP. Subsequently, these AMP can be further hydrolyzed into adenosine by CD73(25). Previous studies have indicated that ENTPD1 is overexpressed in some blood and solid tumor cells, such as acute B lymphoblastic leukemia (B-ALL), acute myeloid leukemia (AML), NSCLC, and hepatocellular carcinoma, promoting tumor cell growth (26-28). Moreover, ENTPD1 has been shown to be overexpressed in cytarabine resistant AML cells (24). Consistent with previous studies, we also observed that ENTPD1 was upregulated in osimertinib-resistant cells compared to sensitive cells (Figure 5A). Using TCGA data, we found that higher ENTPD1 expression was significantly associated with poorer OS and PFS in lung cancer patients (Figure 5B).

Besides tumor cell growth-promoting activity, ENTPD1 also plays a vital role in regulating the anti-tumor immune response. Extracellular adenosine produced by ENTPD1 can bind to adenosine receptors, which are expressed in some immune cells, including regulatory T cells (Tregs) and myeloid-derived suppressor cells (MDSCs). Acting through adenosine receptors, extracellular adenosine can help tumor cells to

escape from host immunosurveillance by promoting the generation of Tregs and MDSCs, and contributing to their immunosuppressive properties (29,30). As previous studies suggested, the densities of tumor-infiltrating Tregs and MDSCs are correlated with tumor stage, and can be used to predict the patient outcomes in various types of cancer (31,32). Therefore, we used TISIDB database to analyze the correlation between *ENTPD1* level and the abundance of tumor-infiltrating Tregs and MDSCs. Our results showed that both Tregs and MDSCs abundances were positively related to ENTPD1 expression in both LUAD and LUSC samples (Figure 5C and 5D), which implicates that ENTPD1 can serve as an important tumor immunosurppressive molecule in NSCLC. To verify whether ENTPD1 expression could affect patient outcomes because of tumor-infiltrating Tregs and MDSCs, we conducted an analysis of the prognostic value of ENTPD1 expression in lung cancer patients based on the tumor infiltration of Tregs and MDSCs. As a result, high ENTPD1 expression in both enriched Tregs cohort and enriched MDSCs cohort was significantly associated with a poor prognosis (all $P < 0.05$) (Figure 5E and 5F). Thus, ENTPD1 may affect the prognosis of NSCLC patients at least through two coordinated mechanisms, one is directly promoting the growth of NSCLC cells, the other is regulating tumor infiltration of Tregs and MDSCs.

To verify whether lnc-TMEM132D-AS1 can modulate the expression of ENTPD1, we silenced the lnc-TMEM132D-AS1 level in osimertinib-resistant HCC827/OR cells, and found that lnc-TMEM132D-AS1 knockdown could significantly decrease the mRNA level of *ENTPD1* (Figure 5G). According to our lnc-TMEM132D-AS1-miRNA-mRNA network, *ENTPD1* was a target of four miRNAs, hsa-miR-16-5p, hsa-miR-195-5p, hsa-miR-424-5p, and hsa-miR-497-5p, which potentially binding to lnc-TMEM132D-AS1. After lnc-TMEM132D-AS1 knockdown, we found that the expression of hsa-miR-16-5p and hsa-miR-195-5P markedly increased, indicating that lnc-TMEM132D-AS1 might regulate the expression of ENTPD1 by interacting with hsa-miR-16-5p and hsa-miR-195-5P (Figure 5H). However, the interactions among these molecule need further investigation.

Discussion

Osimertinib was approved by the FDA for the management of patients with metastatic EGFR-T790M NSCLC in 2017. However, almost all the patients will develop acquired resistance in about 10 months (6). Common mechanisms discovered thus far include secondary resistance mechanisms that interact with osimertinib's binding to its primary site of action such as development of C797S mutation, and activation of alternative signaling pathways independent of osimertinib's binding site (33). Unfortunately, these mechanisms cannot account for all cases. Moreover, these acquired resistance-related molecules cannot be conveniently monitored during treatment, because taking tissue biopsy is generally an invasive procedure. In such circumstances, lncRNAs hold strong promise as novel biomarkers and therapeutic targets to overcome osimertinib resistance. Accumulating evidence has shown that lncRNAs participate in sensitizing or de-sensitizing cancer cells to chemical drugs during cancer therapeutics (34). Besides, the level of serum lncRNAs can be easily dynamically-monitored and used as ideal non-invasive biomarkers (35).

In this study, we first explored the differential expressed lncRNAs between osimertinib-sensitive and -resistant NSCLC cell lines using RNA-Seq. Our results showed that although thousands of lncRNAs were detected, of which hundreds were differentially expressed in each pair of cell lines, only 32 lncRNAs showed a consistent direction of differential expression across two cell line pairs. Previous studies have shown that CRNDE, MSTRG.292666.16, and HIF1A-AS2 were upregulated in NSCLC cells with acquired resistance to osimertinib, but in our present work, we observed inconsistent results. Both CRNDE and HIF1A-AS2 were commonly downregulated in two resistant cell lines compared with their parental sensitive cells, and these alterations did not reach statistical significance. MSTRG.292666.16 was not detected in any of these lines. These discrepancies might be due to the different cell lines used and the heterogeneous nature of tumors. After qPCR verification, we found lnc-TMEM132D-AS1 was significantly upregulated in NSCLC cell lines as well as in the plasma of patients with acquired resistance to osimertinib. Lnc-TMEM132D-AS1 is located on chromosome 12, and oriented in antisense direction with respect to the *TMEM132D* gene. *TMEM132D* is a human gene identified with multiple risk alleles for panic disorders, anxiety and major depressive disorders, but its actual role is yet not fully understood (36).

Here, we present the first study investigating the function of lnc-TMEM132D-AS1 in acquired resistance to osimertinib in NSCLC. We identified that lnc-TMEM132D-AS1 was significantly upregulated in NSCLC cell lines as well as in the plasma of patients with acquired resistance to osimertinib. A similar result was obtained from TCGA database, indicating that lnc-TMEM132D-AS1 was overexpressed in lung cancer tissues, and its expression was negatively correlated with clinical outcome in lung cancer patients. Thus, lnc-TMEM132D-AS1 may play an unignorable role in the regulation of proliferation, differentiation and chemosensitivity of lung tumor cells. As expected, lnc-TMEM132D-AS1 knockdown resulted in an increased sensitivity of osimertinib-resistant NSCLC cells to osimertinib, but it could not bring back these resistant cells to the sensitive level of their parental sensitive cells. This happens because the acquired osimertinib resistance is a multi-factorial phenomenon, the influence of other mechanisms cannot be ruled out in this study.

Considering that lnc-TMEM132D-AS1 was found to be mainly localized in the cytoplasm, we supposed it might act as a sponge of miRNAs. Therefore, we constructed the lnc-TMEM132D-AS1-miRNA-mRNA interaction network to explore the potential molecular mechanisms of lnc-TMEM132D-AS1. A total of 125 miRNAs and 162 target mRNAs were included in this network, providing a global overview of possible targets of lnc-TMEM132D-AS1 in NSCLC cells. GO and KEGG pathway analyses for these target mRNAs were conducted to investigate the probable functions and potential pathways regulated by lnc-TMEM132D-AS1. Moreover, we systemically analyzed interactions among these target mRNAs by constructing a PPI network, and identified the top 10 hub genes. Among these hub genes, ENTPD1 aroused our interest, because it was predicted to take part in several GO terms, such as immune response, extracellular environment, as well as ATP binding.

Adenosine and ATP are normally present at very low levels in extracellular fluids. Inflammation, ischemia, or cancer can lead to the release of high levels of ATP through a variety of mechanisms, including

transporter- or channel-mediated release, active vesicular exocytosis, and direct release through mechanical stress or cell destruction (37). As a rate-limiting enzyme in the hydrolysis of extracellular ATP, ENTPD1 participates in the generation of adenosine (38). Since the last decade, accumulating evidence has highlighted the role of ENTPD1 in the promotion of tumor cell growth, and elevated ENTPD1 expression has been shown to be an independent poor prognostic factor in various types of cancer, such as NSCLC, hepatocellular carcinoma, ovarian cancer, gastric cancer, as well as breast cancer (39). The precise mechanisms underlying this observation are far from being fully understood, but can be partially explained by its ATP hydrolysis activity. Previous research has indicated that extracellular ATP exerts antitumor activity by directly inhibiting cell proliferation and promoting cancer cell death. While ENTPD1 can quickly metabolize extracellular ATP to AMP, and protect tumor cells from high levels of extracellular ATP (40). Moreover, ENTPD1 has also been shown to promote cytarabine resistance by enhancing mitochondrial activity and biogenesis in AML (24).

Recently, the role of ENTPD1 in regulating tumor immunity is emerging. Tregs and MDSCs are two major immunosuppressive cell populations in tumor environment. Previous reports have shown that extracellular adenosine can bind to the adenosine A_{2A} receptor ($A_{2A}R$) expressed in Tregs, leading to the increased generation of Tregs and decreased Th17 differentiation (30). Similarly, extracellular adenosine also contributes to the enhanced infiltration and accumulation of MDSCs in tumor environment after binding with $A_{2B}R$ (31). As expected, using TISIDB database, we found that both Tregs and MDSCs abundances were positively related to ENTPD1 expression in lung cancer tissues, and high ENTPD1 expression in both enriched Tregs cohort and enriched MDSCs cohort was significantly associated with a poor outcomes. Therefore, ENTPD1 maybe an important factor accounting for the development of NSCLC through at least two mechanisms: promotion of NSCLC cells growth and regulation Tregs and MDSCs infiltration.

Finally, we confirmed that lnc-TMEM132D-AS1 could modulate the expression of ENTPD1, probably through interacting with hsa-miR-16-5p and hsa-miR-195-5P. hsa-miR-195-5p is located at 17p13 with 87 bp in the genome (41). Recent research has indicated that hsa-miR-195-5p is a candidate tumor-suppressor miRNA in various types of cancer. For example, it was found to be significantly down-regulated in NSCLC, thyroid carcinoma, and hepatocellular carcinoma (42–44). Moreover, studies have demonstrated the involvement of hsa-miR-195-5P in acquired bortezomib resistance in multiple myeloma (45). To date, only a few studies have investigated the relationship between hsa-miR-16-5p and cancer. Current research suggests that the expression of hsa-miR-16-5p is dysregulated in epithelial ovarian cancer, triple-negative breast cancer, as well as colon cancer (46–48). However, the interplays among lnc-TMEM132D-AS1, ENTPD1, and hsa-miR-16-5p/hsa-miR-195-5P need further investigation.

Conclusion

In summary, using bioinformatics and molecular biology methods, we found that lnc-TMEM132D-AS1 might serve as a prognostic biomarker and a potential therapeutic target for acquired resistance to

osimertinib in NSCLC. Further investigation could lead to novel insights into the underlying mechanisms of osimertinib resistance in a comprehensive manner.

Declarations

Data availability statement

The original contributions presented in the study are included in the article/Supplementary Material. Further inquiries can be directed to the corresponding author.

Ethnics statment

Studies with human NSCLC specimens have been approved by the Ethics Committee Board of Chongqing Medical University, Chongqing, P.R.China (No. 2017009), and was registered with the Chinese Clinical Trial Registry (No. ChiCTR1800014660). Written informed consents were obtained from all patients.

Conflict of Interest

The authors declare that the research was conducted in the absence of any commercial or financial relationships that could be construed as a potential conflict of interest.

Author Contributions

LW designed the study. NW and QZ conducted the experiments. YH and CW performed data analysis. LW and YL contributed to drafting the article. All authors contributed to the article and approved the submitted version.

Funding

This work was supported by the Natural Science Foundation of China (No. 82073938), the Natural Science Foundation of Chongqing (No. cstc2020jcyj-msxmX0246, cstc2020jcyj-msxmX0258), Scientific and Technological Research Program of Chongqing Municipal Education Commission (No. KJQN201900424), Program for Youth Innovation in Future Medicine, Chongqing Medical University (No.W0093), and Scientific and Technological Research Program of Yuzhong District, Chongqing (No. 20200102).

References

1. Thai AA, Solomon BJ, Sequist LV, Gainor JF, Heist RS. Lung cancer. Lancet (2021) 398:535–554. doi: 10.1016/S0140-6736(21)00312-3
2. Zhang H, Jiang H, Zhu L, Li J, Ma S. Cancer-associated fibroblasts in non-small cell lung cancer: Recent advances and future perspectives. Cancer Letters (2021) 514:38–47. doi: 10.1016/j.canlet.2021.05.009

3. Melosky B, Wheatley-Price P, Juergens RA, Sacher A, Leighl NB, Tsao M-S, Cheema P, Snow S, Liu G, Card PB, et al. The rapidly evolving landscape of novel targeted therapies in advanced non-small cell lung cancer. Lung Cancer (2021) 160:136–151. doi: 10.1016/j.lungcan.2021.06.002
4. Harrison PT, Vyse S, Huang PH. Rare epidermal growth factor receptor (EGFR) mutations in non-small cell lung cancer. Seminars in Cancer Biology (2020) 61:167–179. doi: 10.1016/j.semcancer.2019.09.015
5. Soria J-C, Ohe Y, Vansteenkiste J, Reungwetwattana T, Chewaskulyong B, Lee KH, Dechaphunkul A, Imamura F, Nogami N, Kurata T, et al. Osimertinib in Untreated EGFR-Mutated Advanced Non-Small-Cell Lung Cancer. N Engl J Med (2018) 378:113–125. doi: 10.1056/NEJMoa1713137
6. Tang Z-H, Lu J-J. Osimertinib resistance in non-small cell lung cancer: Mechanisms and therapeutic strategies. Cancer Letters (2018) 420:242–246. doi: 10.1016/j.canlet.2018.02.004
7. He J, Huang Z, Han L, Gong Y, Xie C. Mechanisms and management of 3rd-generation EGFR-TKI resistance in advanced non-small cell lung cancer (Review). International Journal of Oncology (2021) 59: doi: 10.3892/ijo.2021.5270
8. Zhang X, Xie K, Zhou H, Wu Y, Li C, Liu Y, Liu Z, Xu Q, Liu S, Xiao D, et al. Role of non-coding RNAs and RNA modifiers in cancer therapy resistance. Mol Cancer (2020) 19:47. doi: 10.1186/s12943-020-01171-z
9. Takahashi S, Noro R, Seike M, Zeng C, Matsumoto M, Yoshikawa A, Nakamichi S, Sugano T, Hirao M, Matsuda K, et al. Long Non-Coding RNA CRNDE Is Involved in Resistance to EGFR Tyrosine Kinase Inhibitor in EGFR-Mutant Lung Cancer via eIF4A3/MUC1/EGFR Signaling. Int J Mol Sci (2021) 22:4005. doi: 10.3390/ijms22084005
10. Deng Q, Fang Q, Xie B, Sun H, Bao Y, Zhou S. Exosomal long non-coding RNA MSTRG.292666.16 is associated with osimertinib (AZD9291) resistance in non-small cell lung cancer. Aging (Albany NY) (2020) 12:8001–8015. doi: 10.18632/aging.103119
11. Si J, Ma Y, Lv C, Hong Y, Tan H, Yang Y. HIF1A-AS2 induces osimertinib resistance in lung adenocarcinoma patients by regulating the miR-146b-5p/IL-6/STAT3 axis. Mol Ther Nucleic Acids (2021) 26:613–624. doi: 10.1016/j.omtn.2021.09.003
12. Jackman D, Pao W, Riely GJ, Engelman JA, Kris MG, Jänne PA, Lynch T, Johnson BE, Miller VA. Clinical Definition of Acquired Resistance to Epidermal Growth Factor Receptor Tyrosine Kinase Inhibitors in Non–Small-Cell Lung Cancer. J Clin Oncol (2010) 28:357–360. doi: 10.1200/JCO.2009.24.7049
13. Livak KJ, Schmittgen TD. Analysis of Relative Gene Expression Data Using Real-Time Quantitative PCR and the 2 − ΔΔCT Method. Methods (2001) 25:402–408. doi: 10.1006/meth.2001.1262
14. Ru B, Wong CN, Tong Y, Zhong JY, Zhong SSW, Wu WC, Chu KC, Wong CY, Lau CY, Chen I, et al. TISIDB: an integrated repository portal for tumor-immune system interactions. Bioinformatics (2019) 35:4200–4202. doi: 10.1093/bioinformatics/btz210
15. Balsara BR, Testa JR. Chromosomal imbalances in human lung cancer. Oncogene (2002) 21:6877–6883. doi: 10.1038/sj.onc.1205836

16. Brown JD, Mitchell SE, O'Neill RJ. Making a long story short: noncoding RNAs and chromosome change. Heredity (Edinb) (2012) 108:42–49. doi: 10.1038/hdy.2011.104
17. Statello L, Guo C-J, Chen L-L, Huarte M. Gene regulation by long non-coding RNAs and its biological functions. Nat Rev Mol Cell Biol (2021) 22:96–118. doi: 10.1038/s41580-020-00315-9
18. Wang Z, Chen W, Zuo L, Xu M, Wu Y, Huang J, Zhang X, Li Y, Wang J, Chen J, et al. The Fibrillin-1/VEGFR2/STAT2 signaling axis promotes chemoresistance via modulating glycolysis and angiogenesis in ovarian cancer organoids and cells. Cancer Commun (Lond) (2022) 42:245–265. doi: 10.1002/cac2.12274
19. J L, Y J, M L, L D. Tumor suppressor miR–613 induces cisplatin sensitivity in non–small cell lung cancer cells by targeting GJA1. Molecular medicine reports (2021) 23: doi: 10.3892/mmr.2021.12024
20. Luo L, Zhang Z, Qiu N, Ling L, Jia X, Song Y, Li H, Li J, Lyu H, Liu H, et al. Disruption of FOXO3a-miRNA feedback inhibition of IGF2/IGF-1R/IRS1 signaling confers Herceptin resistance in HER2-positive breast cancer. Nat Commun (2021) 12:2699. doi: 10.1038/s41467-021-23052-9
21. Q Y, G W. CircRNA-001241 mediates sorafenib resistance of hepatocellular carcinoma cells by sponging miR-21-5p and regulating TIMP3 expression. Gastroenterologia y hepatologia (2021) doi: 10.1016/j.gastrohep.2021.11.007
22. Zhuang Q-S, Sun X-B, Chong Q-Y, Banerjee A, Zhang M, Wu Z-S, Zhu T, Pandey V, Lobie PE. ARTEMIN Promotes Oncogenicity and Resistance to 5-Fluorouracil in Colorectal Carcinoma by p44/42 MAPK Dependent Expression of CDH2. Front Oncol (2021) 11:712348. doi: 10.3389/fonc.2021.712348
23. Huang J, Yu Q, Zhou Y, Chu Y, Jiang F, Zhu X, Zhang J, Wang Q. A positive feedback loop formed by NGFR and FOXP3 contributes to the resistance of non-small cell lung cancer to icotinib. Transl Cancer Res (2020) 9:1044–1052. doi: 10.21037/tcr.2019.12.60
24. Aroua N, Boet E, Ghisi M, Nicolau-Travers M-L, Saland E, Gwilliam R, de Toni F, Hosseini M, Mouchel P-L, Farge T, et al. Extracellular ATP and CD39 Activate cAMP-Mediated Mitochondrial Stress Response to Promote Cytarabine Resistance in Acute Myeloid LeukemiaExtracellular ATP and Chemoresistance. Cancer Discov (2020) 10:1544–1565. doi: 10.1158/2159-8290.CD-19-1008
25. Canale FP, Ramello MC, Núñez N, Araujo Furlan CL, Bossio SN, Gorosito Serrán M, Tosello Boari J, Del Castillo A, Ledesma M, Sedlik C, et al. CD39 Expression Defines Cell Exhaustion in Tumor-Infiltrating CD8 + T Cells. Cancer Res (2018) 78:115–128. doi: 10.1158/0008-5472.CAN-16-2684
26. Vaisitti T, Arruga F, Guerra G, Deaglio S. Ectonucleotidases in Blood Malignancies: A Tale of Surface Markers and Therapeutic Targets. Front Immunol (2019) 10:2301. doi: 10.3389/fimmu.2019.02301
27. Giatromanolaki A, Kouroupi M, Pouliliou S, Mitrakas A, Hasan F, Pappa A, Koukourakis MI. Ectonucleotidase CD73 and CD39 expression in non-small cell lung cancer relates to hypoxia and immunosuppressive pathways. Life Sci (2020) 259:118389. doi: 10.1016/j.lfs.2020.118389
28. Pang L, Ng KT-P, Liu J, Yeung W-HO, Zhu J, Chiu T-LS, Liu H, Chen Z, Lo C-M, Man K. Plasmacytoid dendritic cells recruited by HIF-1α/eADO/ADORA1 signaling induce immunosuppression in hepatocellular carcinoma. Cancer Letters (2021) 522:80–92. doi: 10.1016/j.canlet.2021.09.022

29. Baghbani E, Noorolyai S, Shanehbandi D, Mokhtarzadeh A, Aghebati-Maleki L, Shahgoli VK, Brunetti O, Rahmani S, Shadbad MA, Baghbanzadeh A, et al. Regulation of immune responses through CD39 and CD73 in cancer: Novel checkpoints. Life Sciences (2021) 282:119826. doi: 10.1016/j.lfs.2021.119826
30. Zarek PE, Huang C-T, Lutz ER, Kowalski J, Horton MR, Linden J, Drake CG, Powell JD. A2A receptor signaling promotes peripheral tolerance by inducing T-cell anergy and the generation of adaptive regulatory T cells. Blood (2008) 111:251–259. doi: 10.1182/blood-2007-03-081646
31. Ryzhov S, Novitskiy SV, Goldstein AE, Biktasova A, Blackburn MR, Biaggioni I, Dikov MM, Feoktistov I. Adenosinergic regulation of the expansion and immunosuppressive activity of CD11b + Gr1 + cells. *Journal of immunology (Baltimore, Md*: 1950) (2011) 187:6120. doi: 10.4049/jimmunol.1101225
32. Shang B, Liu Y, Jiang S, Liu Y. Prognostic value of tumor-infiltrating FoxP3 + regulatory T cells in cancers: a systematic review and meta-analysis. Sci Rep (2015) 5:15179. doi: 10.1038/srep15179
33. Lee C-S, Milone M, Seetharamu N. Osimertinib in EGFR-Mutated Lung Cancer: A Review of the Existing and Emerging Clinical Data. Onco Targets Ther (2021) 14:4579–4597. doi: 10.2147/OTT.S227032
34. Zhou Y, Sun W, Qin Z, Guo S, Kang Y, Zeng S, Yu L. LncRNA regulation: New frontiers in epigenetic solutions to drug chemoresistance. Biochemical Pharmacology (2021) 189:114228. doi: 10.1016/j.bcp.2020.114228
35. Osielska MA, Jagodziński PP. Long non-coding RNA as potential biomarkers in non-small-cell lung cancer: What do we know so far? Biomedicine & Pharmacotherapy (2018) 101:322–333. doi: 10.1016/j.biopha.2018.02.099
36. Wang X, Jiang W, Luo S, Yang X, Wang C, Wang B, Dang Y, Shen Y, Ma DK. The C. elegans homolog of human panic-disorder risk gene TMEM132D orchestrates neuronal morphogenesis through the WAVE-regulatory complex. Mol Brain (2021) 14:54. doi: 10.1186/s13041-021-00767-w
37. Leone RD, Emens LA. Targeting adenosine for cancer immunotherapy. J Immunother Cancer (2018) 6:57. doi: 10.1186/s40425-018-0360-8
38. Wu J, Wang Y-C, Xu W-H, Luo W-J, Wan F-N, Zhang H-L, Ye D-W, Qu Y-Y, Zhu Y-P. High Expression of CD39 is Associated with Poor Prognosis and Immune Infiltrates in Clear Cell Renal Cell Carcinoma. Onco Targets Ther (2020) 13:10453–10464. doi: 10.2147/OTT.S272553
39. Moesta AK, Li X-Y, Smyth MJ. Targeting CD39 in cancer. Nat Rev Immunol (2020) 20:739–755. doi: 10.1038/s41577-020-0376-4
40. Feng L, Sun X, Csizmadia E, Han L, Bian S, Murakami T, Wang X, Robson SC, Wu Y. Vascular. CD39/ENTPD1 directly promotes tumor cell growth by scavenging extracellular adenosine triphosphate. Neoplasia (2011) 13:206–216. doi: 10.1593/neo.101332
41. Li L, Feng T, Zhang W, Gao S, Wang R, Lv W, Zhu T, Yu H, Qian B. MicroRNA Biomarker hsa-miR-195-5p for Detecting the Risk of Lung Cancer. Int J Genomics (2020) 2020:7415909. doi: 10.1155/2020/7415909

42. Liu B, Qu J, Xu F, Guo Y, Wang Y, Yu H, Qian B. MiR-195 suppresses non-small cell lung cancer by targeting CHEK1. *Oncotarget* (2015) 6:9445–9456. doi: 10.18632/oncotarget.3255.
43. Liu D, Li P, Wang X, Wang W. hsa-miR-195-5p inhibits cell proliferation of human thyroid carcinoma cells via modulation of p21/cyclin D1 axis. Transl Cancer Res (2020) 9:5190–5199. doi: 10.21037/tcr-20-1083
44. H X, Yw H, Jy Z, Xm H, Sf L, Yc W, Jj G, Yh S, Cm K, L L, et al. MicroRNA-195-5p acts as an anti-oncogene by targeting PHF19 in hepatocellular carcinoma. Oncology reports (2015) 34: doi: 10.3892/or.2015.3957
45. Zhang L, Pan L, Xiang B, Zhu H, Wu Y, Chen M, Guan P, Zou X, Valencia CA, Dong B, et al. Potential role of exosome-associated microRNA panels and in vivo environment to predict drug resistance for patients with multiple myeloma. Oncotarget (2016) 7:30876–30891. doi: 10.18632/oncotarget.9021
46. Singh R, Som A. Common miRNAs, candidate genes and their interaction network across four subtypes of epithelial ovarian cancer. Bioinformation (2021) 17:748–759. doi: 10.6026/97320630017748
47. Zhang D, An X, Yu H, Li Z. The regulatory effect of 6-TG on lncRNA-miRNA-mRNA ceRNA. network in triple-negative breast cancer cell line. Biosci Rep (2021) 41:BSR20203890. doi: 10.1042/BSR20203890
48. Yang Z, Lu S, Wang Y, Tang H, Wang B, Sun X, Qu J, Rao B. A Novel Defined Necroptosis-Related miRNAs Signature for Predicting the Prognosis of Colon Cancer. Int J Gen Med (2022) 15:555–565. doi: 10.2147/IJGM.S349624

Tables

Table 1
The common differentially expressed lncRNAs within two pairs of osimertinib-sensitive and -resistant NSCLC cell lines.

IDs	Location	Type	Up/Down	HCC827/OR *vs* HCC827		H1975/OR *vs* H1975	
				Fold change	*P* value	Fold change	*P* value
AC006213.3	Chr19	intergenic	Up	38.9144	0.006	20.3347	0.0067
AC107909.1	Chr8	intronic	Up	8.5612	0.0331	48.9881	0.0037
MUC20-OT1	Chr3	intergenic	Up	37.1261	0.0118	17.557	0.0172
LINC01468	Chr10	intergenic	Up	23.2038	0.0211	9.243	0.0236
TMEM132D-AS1	Chr12	intronic	Up	16.8969	0.0097	13.3207	0.0001
ZNF213-AS1	Chr16	intergenic	Up	24.9494	0.0483	4.3313	0.0086
LINC01002	Chr19	intergenic	Up	2.4807	0.0097	26.4895	0.0037
CRIM1-DT	Chr12	intergenic	Up	20.2355	0.0146	8.3187	0.0266
LINC00893	ChrX	intronic	Up	20.11	0.015	2.3101	0.0337
XLOC_003074	Chr12	genic	Up	13.8608	0.0071	5.1011	0.0105
AL391294.1	ChrX	intronic	Up	11.8597	0.0223	6.8149	0.0081
AC090651.1	Chr15	intergenic	Up	7.7829	0.0356	9.243	0.0236
THRB-IT1	Chr12	intronic	Up	9.2815	0.019	7.3944	0.03
AC025171.2	Chr5	intergenic	Up	7.7829	0.0356	7.3944	0.03
AC087430.1	Chr3	intronic	Up	7.0046	0.0384	6.4701	0.0337
AC006064.5	Chr12	intronic	Up	6.1831	0.0093	5.0569	0.0084
CARD8-AS1	Chr19	exotic	Up	4.5953	0.0322	5.0823	0.0173
AL353622.1	Chr1	intergenic	Down	-2.027	0.0058	-2.7471	0.0155
SNHG5	Chr6	intergenic	Down	-2.481	0.0541	-2.7471	0.0263
AC027373.1	Chr8	intergenic	Down	-5.1716	0.0057	-2.453	0.0441
AL024508.2	Chr6	exotic	Down	-5.4948	0.045	-2.4595	0.0364
AL022068.1	Chr6	intronic	Down	-6.4645	0.0062	-4.5452	0.0332
SNHG29	Chr17	intergenic	Down	-5.7447	0.0221	-7.1244	0.0393
ATP2A1-AS1	Chr16	exotic	Down	-5.0484	0.0289	-7.936	0.0126

IDs	Location	Type	Up/Down	HCC827/OR *vs* HCC827		H1975/OR *vs* H1975	
				Fold change	*P* value	Fold change	*P* value
AC103858.2	Chr15	intronic	Down	-9.0502	0.0384	-4.5993	0.0378
SNHG6	Chr8	exotic	Down	-4.8361	0.0257	-12.9863	0.0277
AL136162.1	Chr6	intergenic	Down	-18.1005	0.0296	-2.7828	0.0517
GAS5	Chr1	intergenic	Down	-12.029	0.009	-8.921	0.0001
AC103591.3	Chr1	intronic	Down	-21.848	0.0458	-5.1533	0.0194
AC007952.4	Chr17	intergenic	Down	-21.2649	0.036	-10.0913	0.007
AC051619.7	Chr15	exotic	Down	-29.7365	0.0178	-2.0922	0.0055
LRRC75A-AS1	Chr17	exotic	Down	-11.4094	0.0103	-20.9222	0.0138

Figures

Figure 1

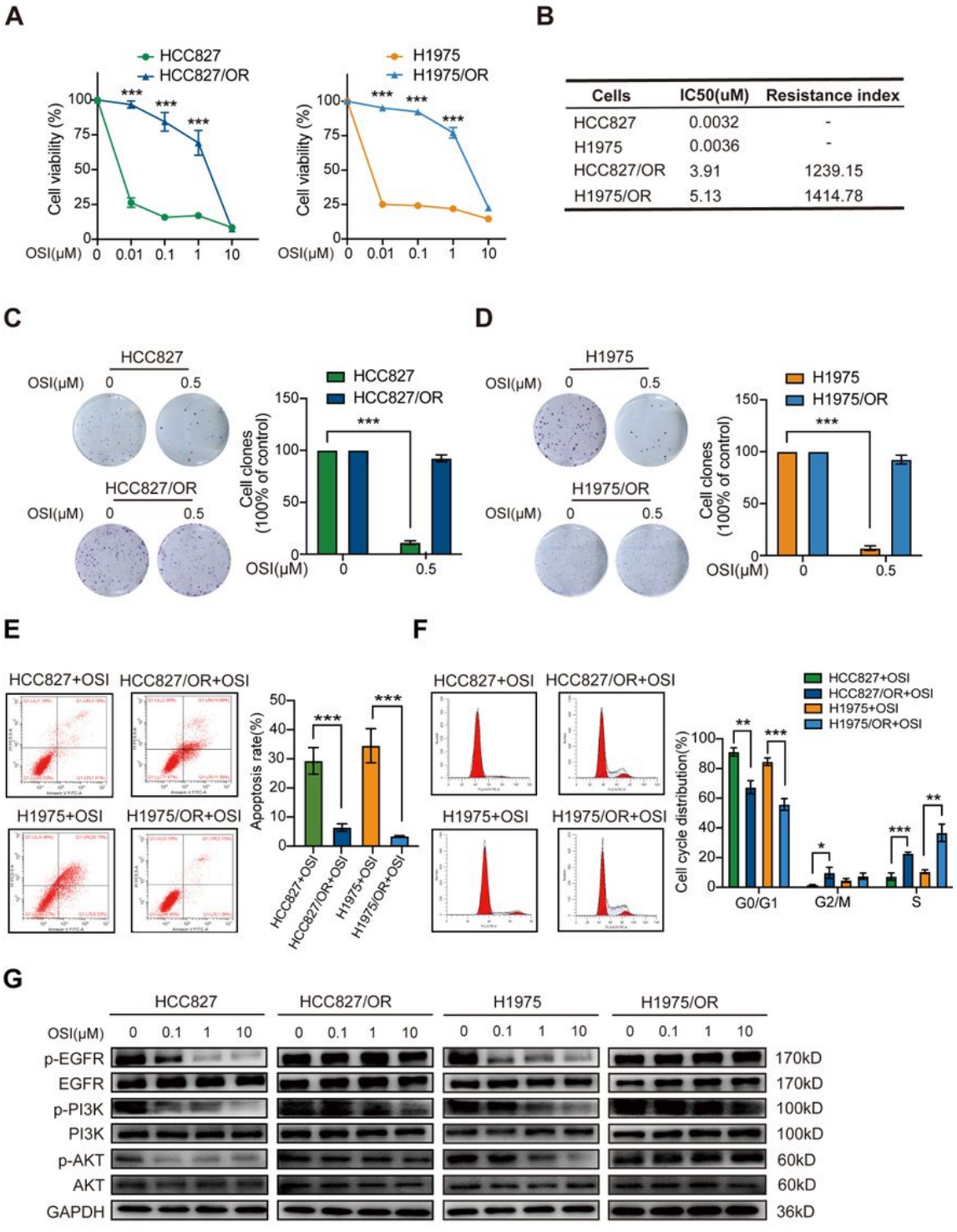

Cells	IC50(uM)	Resistance index
HCC827	0.0032	-
H1975	0.0036	-
HCC827/OR	3.91	1239.15
H1975/OR	5.13	1414.78

Figure 1

Establishment and validation of osimertinib-resistant NSCLC cell lines. (A, B) HCC827/OR, H1975/OR and their parent cells were treated with different concentrations of osimertinib for 72h. CCK-8 assay was used to detect cell viability, the IC_{50} values and resistance indices were calculated. (**C, D)** The colony formation abilities of osimertinib-sensitive and -resistant NSCLC cell lines. (**E, F)** NSCLC cells were treated with 0.5μM osimertinib for 72 h, cell apoptosis and cycle were examined by flow cytometry. (**G)** Activation of

the EGFR signaling pathway in osimertinib-sensitive and -resistant NSCLC cells after osimertinib treatment.*P<0.05, **P<0.01, ***P<0.001.

Figure 2

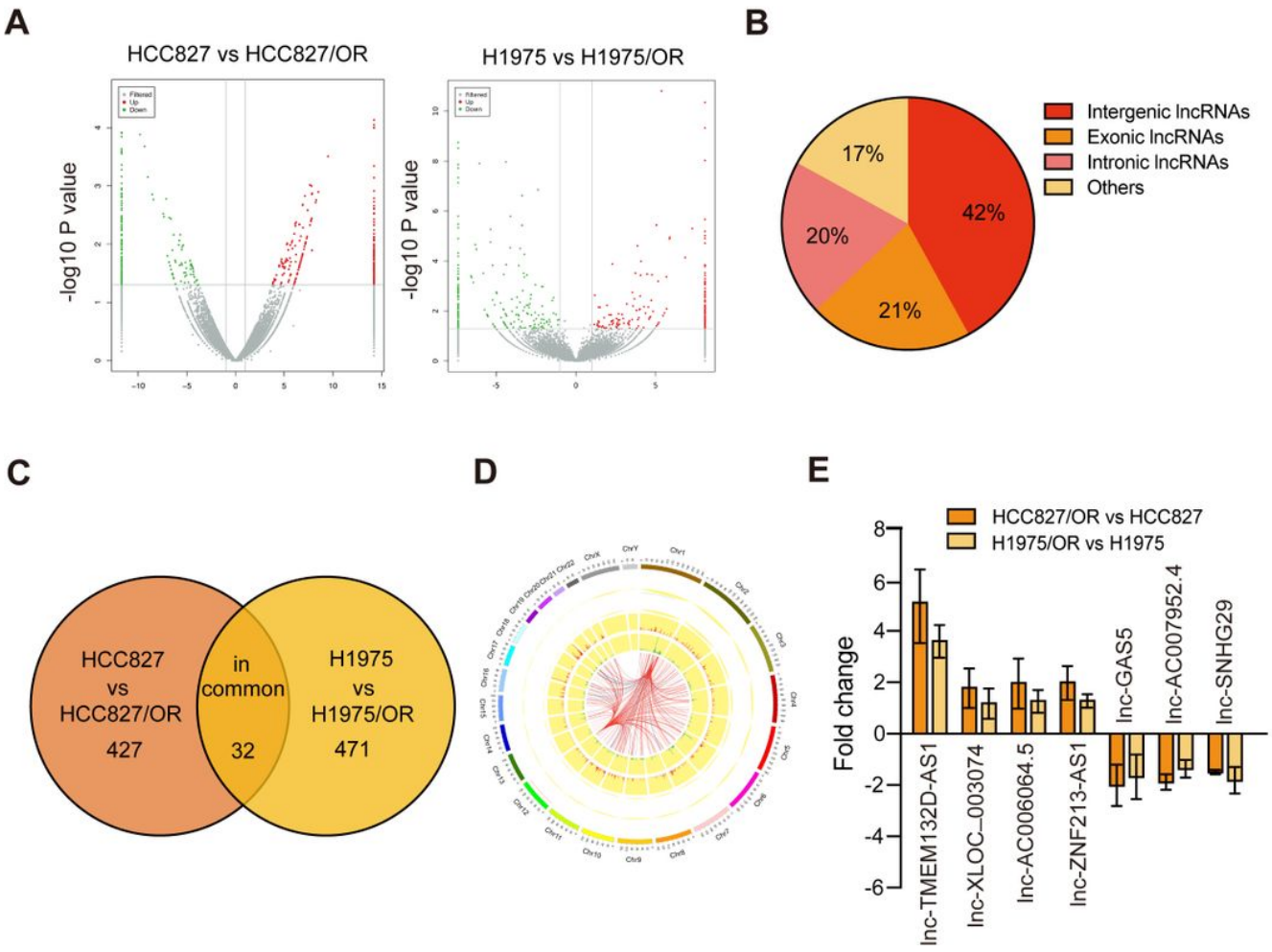

Figure 2

Differentially expressed lncRNAs between osimertinib-sensitive and -resistant NSCLC cell lines. (A) Volcano plots showing the differential lncRNAs expression profiles between osimertinib-sensitive and -resistant NSCLC cell lines. **(B)** Types of the identified lncRNAs. **(C)** Venn diagram showing the number of differentially expressed lncRNAs overlapping between the two comparisons. **(D)** The differentially expressed lncRNAs were enriched by a chromosomal localization. **(E)** qPCR validation of expression of the seven selected lncRNAs.

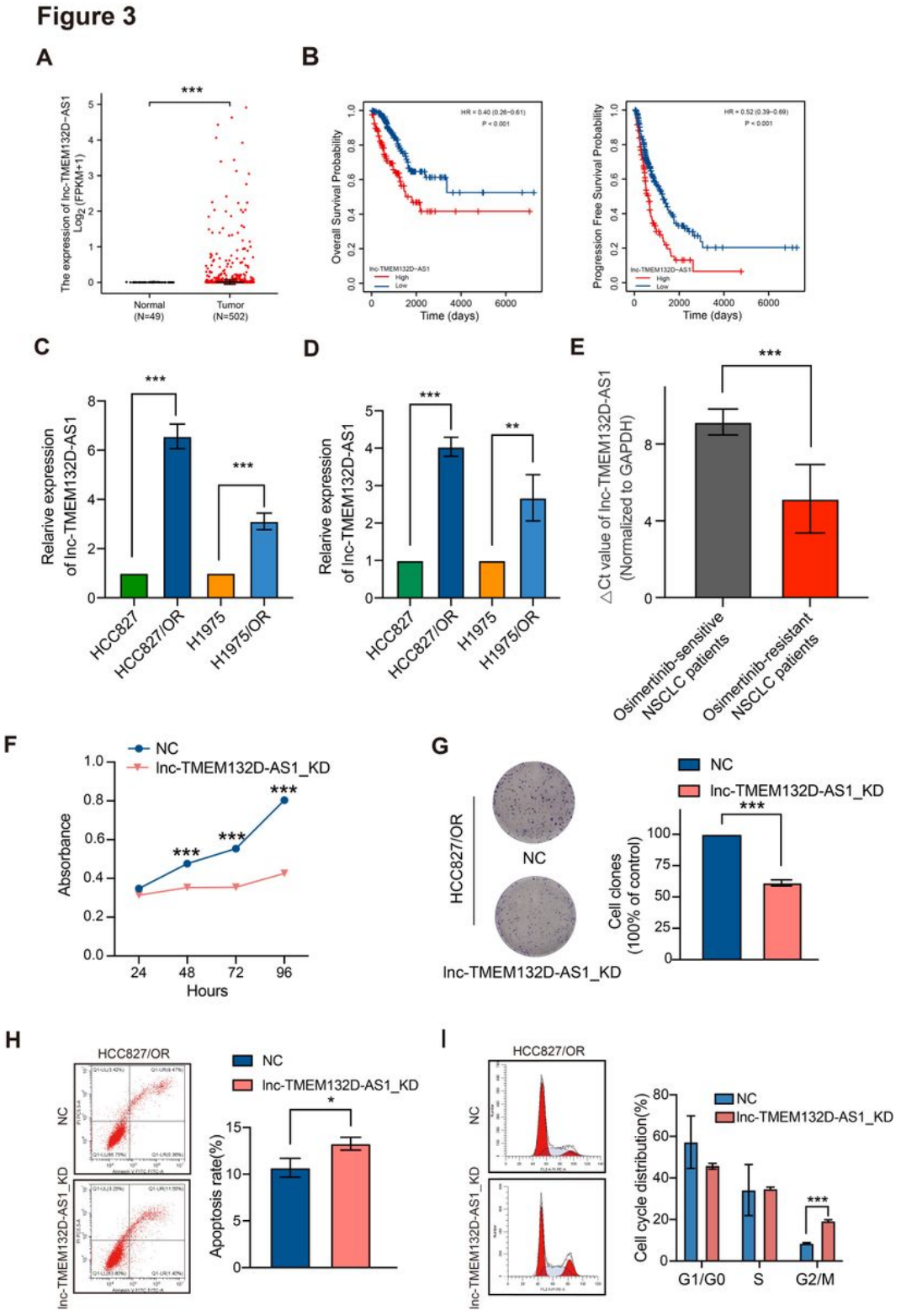

Figure 3

Lnc-TMEM132D-AS1 reduces osimertinib sensitivity in NSCLC cells. (A) Lnc-TMEM132D-AS1 was significantly overexpressed in lung cancer tissues based on TCGA database. (**B**) The expression of lnc-TMEM132D-AS1 was correlated with the clinical outcome of patients with lung cancer. **(C, D)** The expression of lnc-TMEM132D-AS1 in both the whole-cell lysates and the culture supernatants of osimertinib-sensitive and -resistant NSCLC cells. (**E**) The expression of lnc-TMEM132D-AS1 in the plasma

of osimertinib-sensitive and -resistant NSCLC patients. (**F, G**) Lnc-TMEM132D-AS1 knockdown decreased the cell viability and colony formation of HCC827/OR cells after osimertinib treatment. (**H, I**) Lnc-TMEM132D-AS1 knockdown induced the cell apoptosis and M2/G-phase cell cycle arrest in HCC827/OR cells after osimertinib treatment. $^{*}P<0.05$, $^{**}P<0.01$, $^{***}P<0.001$.

Figure 4

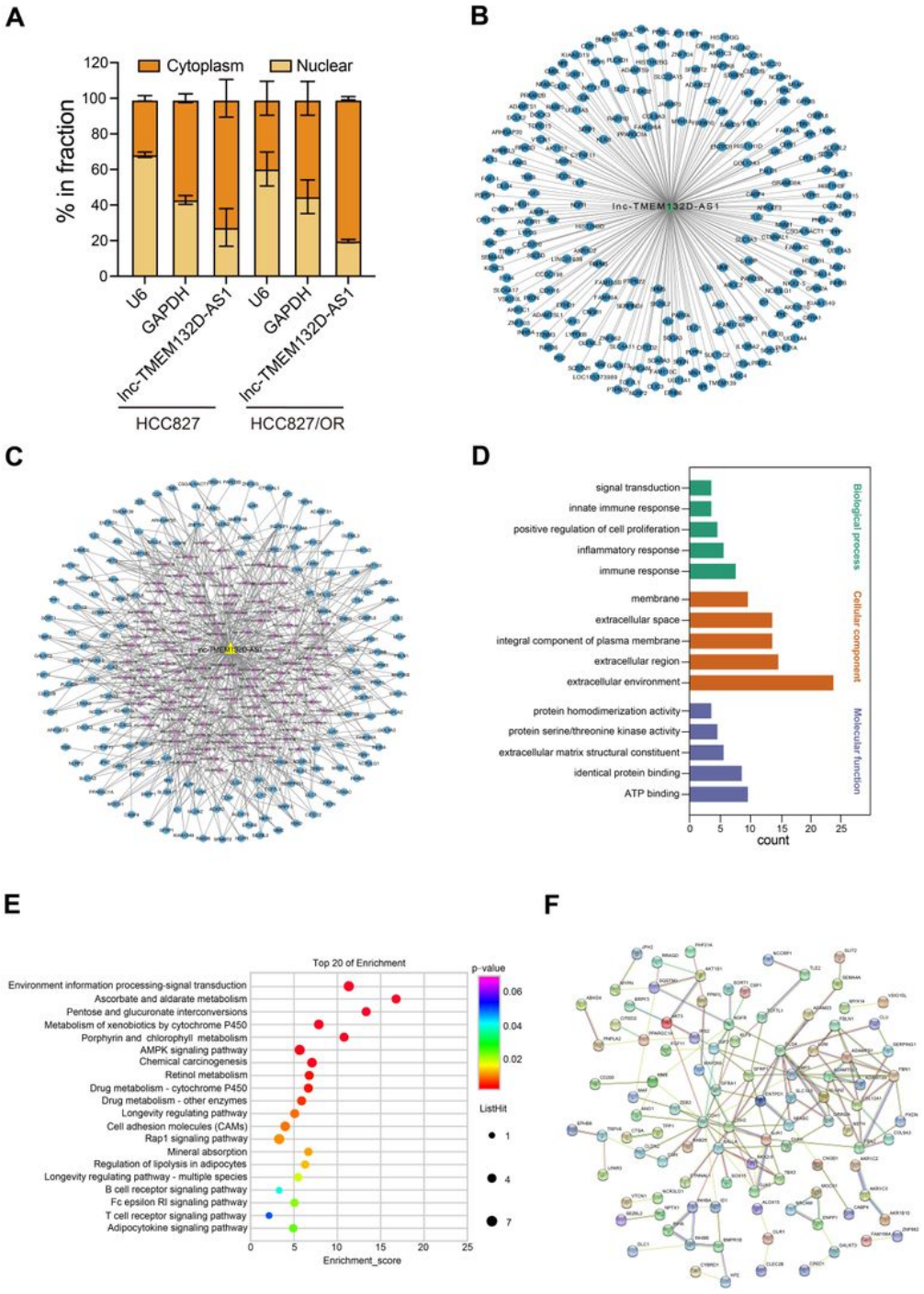

Exploration of the potential mechanisms of lnc-TMEM132D-AS1 in osimertinib resistance. (A) The expression of lnc-TMEM132D-AS1 in either the cytoplasm or nucleus of NSCLC cell lines. **(B)** Lnc-TMEM132D-AS1-mRNA co-expression network. Green triangle node indicates lnc-TMEM132D-AS1, and blue circular nodes indicate mRNAs. **(C)** Construction of the lnc-TMEM132D-AS1-miRNA-mRNA interaction network. Yellow triangle node represents lnc-TMEM132D-AS1, purple diamond nodes represent miRNAs, blue circular nodes represent mRNAs. **(D)** The top 15 GO terms for the 162 mRNAs from lnc-TMEM132D-AS1-miRNA-mRNA interaction network. The horizontal axis shows the name of the GO entry, and the vertical axis shows the -log10 *P* value. **(E)** Bubble maps for KEGG analysis of the 162 mRNAs from lnc-TMEM132D-AS1-miRNA-mRNA interaction network associated with significantly enriched signaling pathways. The X-axis in the graph represents the ratio of the enriched differential gene to the background gene of the pathway. The Y-axis shows the name of the statistically enriched pathway. The size of the dots in the graph indicates the number of differential genes enriched. **(F)** PPI network for the 162 mRNAs from the lnc-TMEM132D-AS1-miRNA-mRNA interaction network. Circular node represents a single mRNA. The edges between nodes indicate the confidence score between them, where the width of the edge is positively associated with the PPI confidence score.

Figure 5

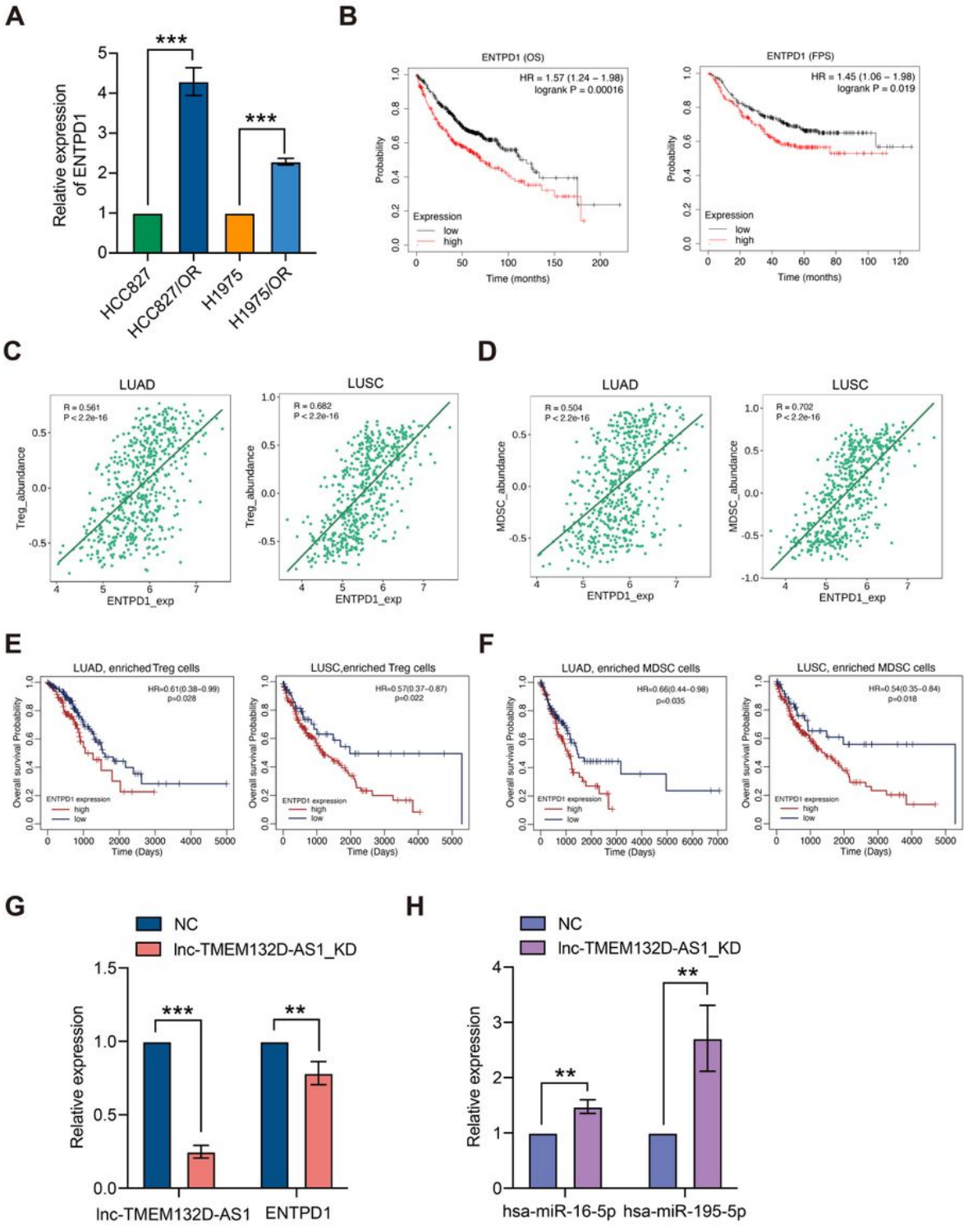

Figure 5

ENTPD1 is a target gene of lnc-TMEM132D-AS1, and correlated with tumor-infiltrating immunosuppressive cells and poor prognosis in patients with NSCLC. (A) The expression of ENTPD1 was significantly higher in osimertinib-resistant NSCLC cells compared to sensitive cells. **(B)** Higher ENTPD1 expression was significantly associated with poorer OS and PFS in lung cancer patients based on TCGA database. **(C, D)** ENTPD1 expression in LUAD and LUSC tissues was positively correlate with the

abundance of tumor-infiltrating Tregs and MDSCs. **(E, F)** High ENTPD1 expression in both enriched Tregs cohort and enriched MDSCs cohort was significantly associated with a poor prognosis. **(G)** The mRNA level of ENTPD1 was decreased after lnc-TMEM132D-AS1 knockdown in HCC827/OR cells. **(H)** The expression levels of hsa-miR-16-5p and hsa-miR-195-5P were increased after lnc-TMEM132D-AS1 knockdown in HCC827/OR cells. $^{**}P<0.01$, $^{***}P<0.001$.

Supplementary Files

This is a list of supplementary files associated with this preprint. Click to download.

- TableS1.docx
- TableS2.docx